TRI-PP-95-11
March 1995

Properties of the TRIUMF neutron beam*

L. Gan[1], R. Abegg[2,3], A.R. Berdoz[1], J. Birchall[1], J.R. Campbell[1], C.A. Davis[1,2], P.W. Green[2,3], L.G. Greeniaus[2,3], R. Helmer[2,3], E. Korkmaz†, L. Lee[1], J. Li[3], C.A. Miller[2,3], A.K. Opper[3], S.A. Page[1], W.D. Ramsay[1], J. Soukup[3], W.T.H. van Oers[1], J. Zhao‡

[1] *University of Manitoba, Department of Physics, Winnipeg, Manitoba, Canada R3T 2N2*

[2] *TRIUMF, 4004 Wesbrook Mall, Vancouver, B.C., Canada V6T 2A3*

[3] *University of Alberta, Department of Physics, Edmonton, Alberta, Canada T6G 2N5*

ABSTRACT

Properties of the TRIUMF neutron beam (4A/2) are presented and compared with a Monte Carlo prediction. The beam intensity profile, energy spectrum and polarization are predicted taking into account the beam line geometry, energy losses in the LD_2 production target, the properties of the $\vec{p}d \rightarrow \vec{n}pp$ reaction, and the scattering of neutrons from the collimator walls. The results allow for improved corrections to systematic errors in a number of TRIUMF neutron experiments.

(Submitted to Nucl. Instr. and Meth. in Phys. Res.)

*Supported in part by the Natural Sciences and Engineering Research Council of Canada.

†Presently at: Department of Physics, University of Northern British Columbia, 3333 University Way, Prince George, B.C., Canada V2N 4Z9

‡Presently at: Laboratory for Nuclear Science, MIT, 77 Massachusetts Ave., Cambridge, MA 02139, U.S.A.

1. Introduction

The neutron beam facility at TRIUMF [1] has served in a number of neutron-proton scattering investigations, most recently: investigations of the isospin mixing, charge symmetry breaking (CSB) component of the strong force [2] [3] [4] [5]; a measurement of the spin correlation parameter A_{NN} and analyzing power [6] [7]; a measurement of the ratio of spin transfer parameters D_t/R_t [8]; pion production in $np \rightarrow pp\pi^-$ [9]; and a measurement of the zero-crossing angle of the analyzing power below 300 MeV [10]. The np elastic scattering experiments have made use of the basic equipment (modified over time) assembled for the first CSB experiment [11]. Data collected with this equipment and the beam profile monitor discussed in ref. [1] are here compared to the predictions of a Monte Carlo simulation that takes into account the geometry of the neutron collimator, the position of the neutron production (LD_2) target and experimental equipment, the physics of the neutron production reaction $\vec{p}d \rightarrow \vec{n}pp$, and the scattering of the neutrons from the walls of the collimator. Information on the horizontal position profile, neutron energy profile, and polarization (spin transfer) profile are derived from the simulation and, where possible, compared to measurements. Good knowledge of these beam properties is essential for understanding the data of sensitive experiments, especially the CSB experiments mentioned above.

2. Neutron production

The TRIUMF neutron facility makes use of the sideways-to-sideways spin transfer coefficient, R_t or K_{ss}, in $(\vec{p},\vec{n})$ scattering at 9°, which is large and negative over all TRIUMF beam energies. Specifically, the spin transfer coefficient, r_t or $K_{ss}(D)$, of this reaction on deuterium is used. Bugg and Wilkin [12] calculate the neutron spectrum from $d(\vec{p},\vec{n})pp$, and how the spin-transfer parameters vary across the spectrum for several incident proton energies. Predictions for $\Delta K_{ss} = K_{ss}(H) - K_{ss}(D) = R_t - r_t$ (see table 2 of ref. [12]) tend to be positive at 9° and, therefore, enhance the free np value of K_{ss} spin transfer.

The values for ΔK_{ss} [12] and recent values for K_{ss} (R_t) from SAID [13] were parametrized as functions of incident proton energy and outgoing neutron energy. The probability of a neutron scattering around 9° along the 217 mm LD_2 target length, corrected for the proton energy loss to that point, was used to randomly choose the $d(\vec{p},\vec{n})pp$ reaction point for the neutron and the value of the outgoing neutron energy with the appropriate value for r_t (and r'_t) assigned. The energy loss must take into account the average density of the deuterium (which is monitored periodically during experiments). Calculations involving convection of the liquid deuterium in the target indicate that, for the usual beam intensities (1 to 2 μA), changes of the liquid deuterium temperature, and therefore density, were negligible ($< 0.2°$), along the path of the proton beam.

3. Neutron collimator

As reported in ref. [1], the neutron beam collimator is mounted in one of several pipes ("ports") built into a shielding box at 3° intervals from −3° to 27° (the unused ports being entirely filled with steel plugs) on the left-hand side of the TRIUMF 4A beam line, see fig. 1. In practice, only the 9° port is used due to the magnitude of the spin transfer parameters discussed in the previous section. The neutron collimation is defined by a set of 305 mm long cylindrical steel inserts, each with a rectangular cross-section aperture, stepped in progressively larger sizes, producing an approximation to a taper. The dimensions of these collimator inserts were adapted to the requirements of the experiments and are listed in table 1. The steel cylinders, of two different diameters (this is because the pipes are stepped - with a gradual transition region - in two different diameters), fit together by pegs on the trailing end of each cylinder mating to a hole in the following cylinder. The primary proton beam, upon exiting the LD_2 target, which is nominally centered along the lines of the collimator ports, passes through a dipole bending magnet (4AB2, 'Clearing Magnet'), through a collimator, and is directed into a beam dump that is well shielded from the experimental area. The neutrons produced in the LD_2 target at about 9° pass through a thin stainless steel wall in the 4AB2 vacuum box and traverse a corner of the 4AB2 field before entering the 9° port collimator.

The Monte Carlo program tracks the neutrons from the production target, taking into consideration the probability that neutrons hitting the sides of the collimator scatter at a small enough angle that they can then pass through the remainder of the collimator. These scattering probabilities, both elastic and inelastic, are based on the cross-section predictions of Pearlstein [14] for intermediate energy nucleons scattering off iron. The surviving neutrons are then followed through to either the experimental target location or the beam profile monitor location. An ensemble of such events, typically $\sim 10^6$, with position, energy, and polarization (spin transfer) values was then used for comparison to measured beam characteristics as discussed below.

4. Neutron beam profile

Fig. 2 shows a comparison between the Monte Carlo predictions for the neutron beam intensity profile and data from a recent experiment [5]. The general shape is trapezoidal, as expected from the basic collimation geometry. There is, however, a slight roll-off of the flat-top of the profile on the left-hand (+) side and a displacement of the beam profile some 8 mm to the right of the nominal center-line. This discrepancy was reproduced very well by the Monte Carlo by displacing the LD_2 target by 6 mm upstream from the point at which the nominal 9° collimator center-line intersects the proton (4A/1) beam center-line. This position error was later confirmed by a measurement to be 6.2 ± 3.9 mm. The 'wings' of the beam are also predicted by Monte Carlo (in the experimental data they are cut off by the acceptance of the neutron profile monitor) and are solely due to the scattered neutrons. The disagreement

with the data around 0 mm arises from the experimental target (which was not included in the Monte Carlo) 'shadow' in the beam. The small difference between prediction and data for the side-slopes may arise from a slight misalignment of some material along the beam path, most likely the 'anti-scattering' collimator in the first neutron spin-precession dipole, labelled "V" in fig. 1, or from inaccurate information as to the distance of the profile monitor from the collimator. The higher than predicted 'wing' on the left supports the former of these conjectures.

5. Neutron beam energy

The majority of recent experiments involved the elastic scattering of neutrons from a hydrogenous target. Time-of-flight (TOF) of both scattered neutron and recoil proton were measured [11], as was the TOF of the incident neutron relative to the cyclotron RF (i.e., arrival of proton bunch time at the LD_2 target). This information permits two independent measurements of the total incident neutron energy. A cut on the difference between these two measurements, ΔE, along with cuts on opening angle, coplanarity, and momentum balance, define the elastic scattered np events. For this section data accumulated for the experiment of ref. [10] are used.

The measurement of the recoil proton TOF was started by a 1.6 mm thick × 130 mm wide × 152 mm high scintillator viewed top and bottom by photomultiplier tubes (PMT's) ~290 mm from the target center. This also served as the start (with suitable corrections for the added proton flight time) for the scattered neutron and the stop of the incident neutron (versus Cyclotron RF). The error in the averaged (both tubes present) proton TOF start counter was independently measured as ~260 ps.

The predicted energy distribution of the neutron beam is shown in fig. 3. The data are from reconstructed neutron elastic scattering events from which the average of the incident and scattered energy is used. As measurements of the neutron energy are affected by various experimental uncertainties, one must fold in these uncertainties by convoluting with the prediction for the neutron energy spectrum a Gaussian shape (in the TOF variable) whose σ can, nonetheless, be reasonably predicted from the difference between the two energy measurements. As well, differential cross-section and efficiency integrated across the acceptance of the detector system [11] must also be taken into account. As the proton TOF start counter effectively provides the start time for the scattered particles' energy measurement and simultaneously the stop time for the incident neutron's energy measurement, its error partially cancels in the energy averaging, and the true σ is somewhat smaller than that determined above from the energy difference. The full cyclotron RF phase acceptance is ~ 35° (4 ns, full width) [15], though the actual time spread of the incident proton beam was usually narrower than this, and long term drifts within the phase acceptance were corrected. Scattered neutron and recoil proton energy uncertainties were also complicated by flight path uncertainties, arising from an uncertainty in the scattering event origin in the target for the neutron and from multiple scattering for the proton. Altogether, these errors translated at the peak of the energy distribution into an

energy σ ranging from 4.9 MeV at $E_n = 175$ MeV to ~9 MeV at $E_n = 261$ MeV. At higher TRIUMF neutron energies, these timing errors begin to dominate the measured neutron energy spectrum, with $\sigma \simeq 20$ MeV at $E_n = 477$ MeV [3]. This folding has been done in the comparison to the data in fig. 3.

The data are reasonably reproduced over the peak by the Monte Carlo simulation, but the tail seems to be higher in reality than predicted. It should be noted that the inclusion of the neutron collimator scattering has no discernable effect on the neutron energy profile because the inelastic differential cross-section by which the neutron would lose only a few 10's of MeV is very small. As the collimation is really quite tight, there is very little latitude for path length variation affecting the apparent energy derived from the TOF of the incident neutron. The contribution to the neutron beam from reactions in the target windows was measured to be ~0.3 – 0.6% of the flux from the deuterium. At lower energies, this contamination in the beam has a polarization of the same sign and at least half the magnitude of neutrons produced from the deuterium itself. The component of the neutron energy profile unexplained by the Monte Carlo that lies within the usual energy cuts (typically ~3 σ down from the peak) is 2 to 5%. These unpredicted neutrons in the tail could possibly arise from neutrons trapped within the LD_2 target cavity that bounce back out the 9° port, most of which would be of lower energy. All of these neutrons would be of somewhat longer flight-path, making the TOF longer and the apparent E_n less; although, for measured E_n much less than true E_n, these would be removed by the ΔE cuts. The probability of nuclear scattering in the LD_2 target into all angles and energies is ~4%, or approximately four orders of magnitude greater than the direct flux down the 9° port (~0.1 msr). Unfortunately, there is no reliable method of modelling this. However, the energy profile is reasonably reproduced provided one accepts a cut on energy not too far down the lower energy side of the peak. As rescattering would tend to sample a broad spectrum in original energy and angle and in spin depolarization with each scattering, it is reasonable to assume an average polarization for such particles $\simeq 0$. In this case, there is no effect on the calculated averaged energy weighted by the square of the polarization, though the average polarization is affected.

The predicted average energy as a function of horizontal position at the experimental target position is shown in fig. 4. There is a flat central region corresponding to the same in the trapezoidal neutron profile (see fig. 2). This is flanked by two sloped regions corresponding the side-slopes of the neutron profile. Their average energy rises (falls) with displacement from beam center as the view through the aperture cuts off more and more of the down-stream (up-stream) part of the LD_2 target. As with the neutron profile, a roll-off from the flat region can be observed at about +30 mm. This arises from the LD_2 target misplacement. The 'wings' of the beam have a discontinuous change relative to the central average because they have scattered from the *opposite* side of the neutron collimator (and have higher or lower energy as per the corresponding neutron energy profile side-slope from which they scattered).

6. Polarization

The incident proton polarization is measured in polarimeters in the 4A beam line [1] [16] [17]. Neutron polarization monitors [1] were used to calibrate the proton precession by a solenoid in the 4A beam line (see fig. 1) and by two neutron spin-precession dipoles ("H" and "V") in the neutron area. The effect of the 4AB2 dipole that bends the proton beam towards the 4A beam dump was also taken into account. The solenoid precesses the proton spin by 90° into the horizontal plane; the vertical-field dipole ("V") and 4AB2 ("Clearing Magnet") align the neutron spin along the beam direction; and the horizontal-field dipole ("H") precesses the neutron spin once again into a vertical direction. These calibrations apply only for the nominal neutron energy. For more refined calculations, it is necessary to calculate the precession as a function of neutron momentum using the initial neutron sideways polarization. This requires knowledge of r_t as a function of the neutron energy from $d(\vec{p},\vec{n})pp$. Such predictions from the Monte Carlo are used to derive the average polarization as a function of energy and position.

Fig. 5 shows the energy dependence of the spin transfer at four incident proton energies.

Conclusion

For analysis of high accuracy neutron scattering experiments, complete knowledge of the properties of the neutron beam is required. Specifically, knowledge of the position of the beam relative to the target and assurance that the target is within the flat central region of the beam profile, and that it is also within the region of flat average energy and polarization as a function of position, are crucial. To calculate the average energy of a polarized neutron beam, the profile must be weighted by the polarization dependence on energy. This is an important consideration for the CSB experiments, as comparisons must be made between polarized and unpolarized neutron beams. This document reports the properties of the TRIUMF neutron beam as compared to Monte Carlo predictions.

Acknowledgements

The authors greatly appreciate: S. Pearlstein for discussions of his program [14]; D.V. Bugg for providing his program reported on in ref. [12]; A.M. Sekulovich and V. Sum for assistance with neutron energy calibrations; and J. Martin and S.D. Reitzner for time resolution studies on the proton TOF start counters.

References

[1] R. Abegg, J. Birchall, E. Cairns, G.H. Coombes, C.A. Davis, N.E. Davison, P.W. Green, L.G. Greeniaus, H.P. Gubler, W.P. Lee, W.J. McDonald, C.A. Miller, G.A. Moss, G.R. Plattner, P.R. Poffenberger, G. Roy, J. Soukup, J.P. Svenne, R. Tkachuk, W.T.H. van Oers and Y.P. Zhang, Nucl. Instr. and Meth. in Phys. Res. A234 (1985) 11.

[2] R. Abegg et al., Phys. Rev. Lett. 56 (1986) 2571.

[3] R. Abegg et al., Phys. Rev. D 39 (1989) 2464.

[4] C.A. Davis et al., "Charge Symmetry Breaking at TRIUMF: Past, Present, and Future" in *High Energy Spin Physics, vol. 1: Conference Report* , Proceedings of the Ninth International Symposium held at Bonn, FRG, 6-15 Sept. 1990, Springer-Verlag, Berlin (1991) 593.

[5] R. Abegg et al., Nucl. Instr. and Meth. in Phys. Res. B79 (1993) 318.

[6] D. Bandyopadhyay et al., Phys. Rev. C 40 (1989) 2684.

[7] R. Abegg et al., Phys. Rev. C 40 (1989) 2406.

[8] R. Abegg et al., Phys. Rev. C 38 (1988) 2173.

[9] M.G. Bachmann et al., Few-Body Systems, Suppl. 7, (1994) 225; P.J. Riley et al., "Measurement of $np \rightarrow pp\pi^-$ at 443 MeV", in proceedings of the *RIKEN International Workshop on Delta Excitation in Nuclei*, H. Toki, M. Ichimura and M. Ishihara, eds., (World Scientific, 1993) 21.

[10] C.A. Davis, in Proceedings of High Energy Spin Physics-1994, ed. E.J. Stephenson, AIP Conference Proceedings, to be published.

[11] R. Abegg et al., Nucl. Instr. and Meth. in Phys. Res. A234 (1985) 20.

[12] D.V. Bugg and C. Wilkin, Nucl. Phys. A467 (1987) 575.

[13] R. Arndt, Interactive Dial-in program SAID, SP94 solution.

[14] S. Pearlstein, The Astrophysical Journal 346 (1989) 1049; medium energy cross-section code PNEM; and private communication.

[15] W.D. Ramsay, N.E. Davison, D.A. Hutcheon, R. Laxdal, and J. Pearson, Nucl. Instr. and Meth. in Phys. Res. A237 (1993) 265.

[16] R. Abegg and R. Schubank, TRIUMF Design Note TRI-DN-87-17 (1987), unpublished.

[17] L.G. Greeniaus and J. Soukup, TRIUMF Design Note TRI-DNA-81-1 (1981), unpublished.

Table 1.
Dimensions of the cylinder holes that define the neutron collimation, as described in the text.

Section #	Diameter (mm)	Width (mm)	Height (mm) >Nov. 1991	Height (mm) <Nov. 1991
1	102	39.1	22.5	18.2
2	102	39.8	24.1	19.6
3	102	40.5	25.6	21.0
4	102	41.2	27.0	22.4
5	102	41.9	28.5	23.8
6	102	42.6	30.1	25.2
7	127	43.3	31.6	26.6
8	127	44.0	33.0	28.0
9	127	44.7	34.4	29.4
10	127	45.4	35.9	30.8
11	127	46.1	37.3	32.2

Figures

1. A schematic representation of the TRIUMF 4A (4A/1 and 4A/2) beam line.

2. A comparison of the Monte Carlo prediction (solid curve) to the measured neutron profile monitor data for the horizontal profile for the CSB experiment [5]. The slight depression at the center of the data is from the experimental target (not included in the Monte Carlo). In keeping with the normal convention, left of beam looking downstream is defined as positive.

3. Neutron spectrum as a function of energy for data from ref. [10] at: (*a*) E_p = 192 MeV; and (*b*) E_p = 280 MeV. The open symbols indicate the neutron spectrum as predicted from the Monte Carlo simulation. The solid line indicates this spectrum convoluted with a Gaussian (in the TOF domain) whose parameters are derived from the $\Delta E = E_{scat} - E_{inc}$ information. This has been normalized to the data (solid symbols) derived from the average of measurements of E_{scat} and E_{inc}. These energies were chosen to demonstrate the shape of the spectrum due to the predictions of ref. [12] because above this the uncertainty in the TOF measurements dominates the shape. The flatness at the peak apparent in (*b*) may arise from the phase (timing) width of the extracted proton beam, which is not necessarily Gaussian.

4. Average energy as a function of the horizontal position at the experimental target location for E_p = 192 MeV as predicted by the Monte Carlo simulation.

5. Neutron energy profiles (a) and spin transfer, r_t, (b) as a function of neutron energy at four incident proton energies: 192.1 MeV (solid squares), 235.0 MeV (open triangles), 279.8 MeV (solid diamonds), and 369.0 MeV (open circles).

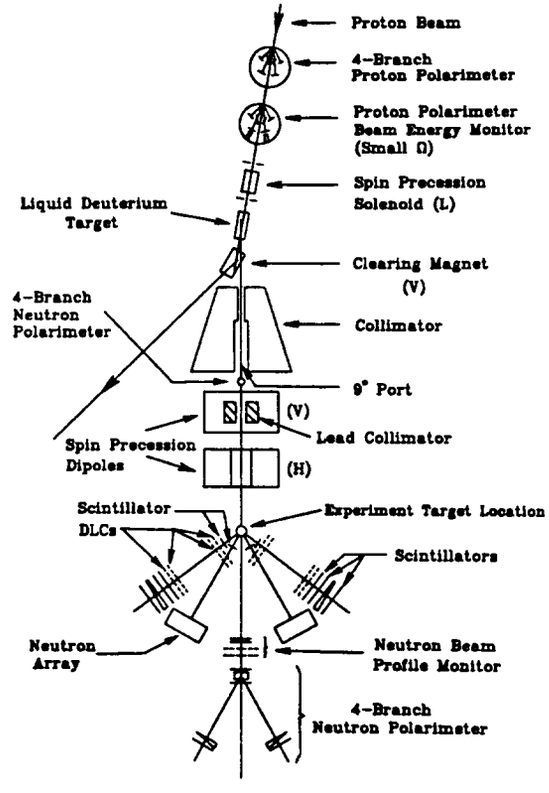

Fig. 1

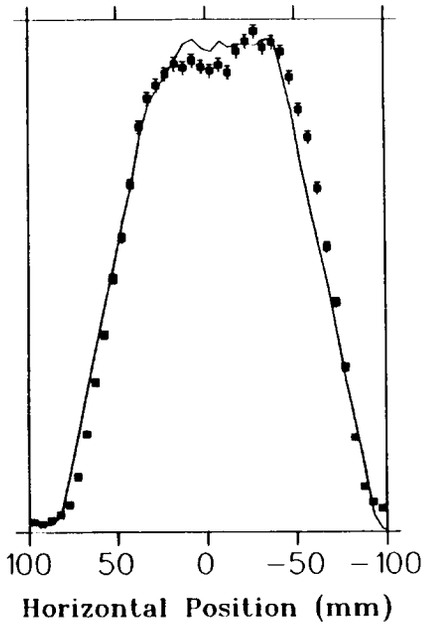

Fig. 2

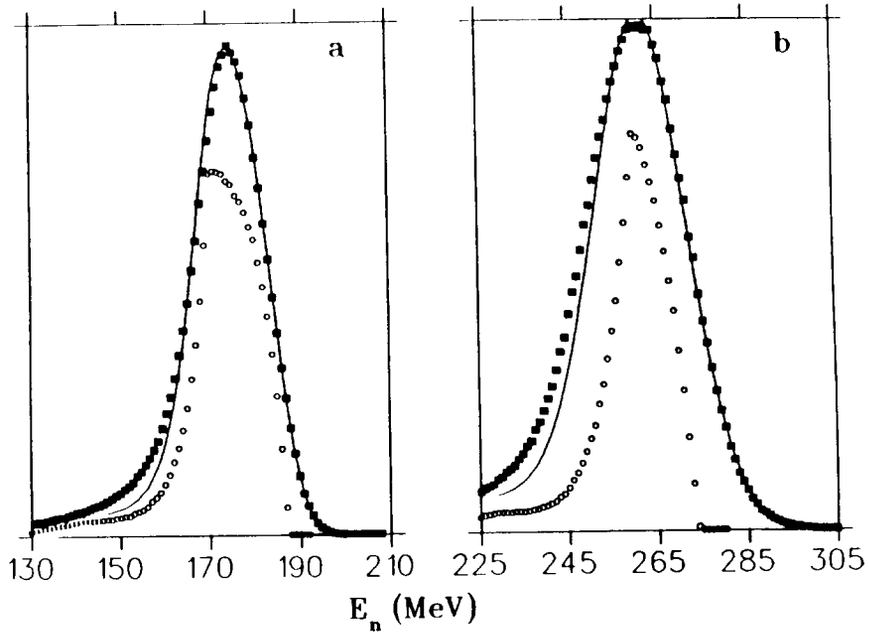

Fig. 3

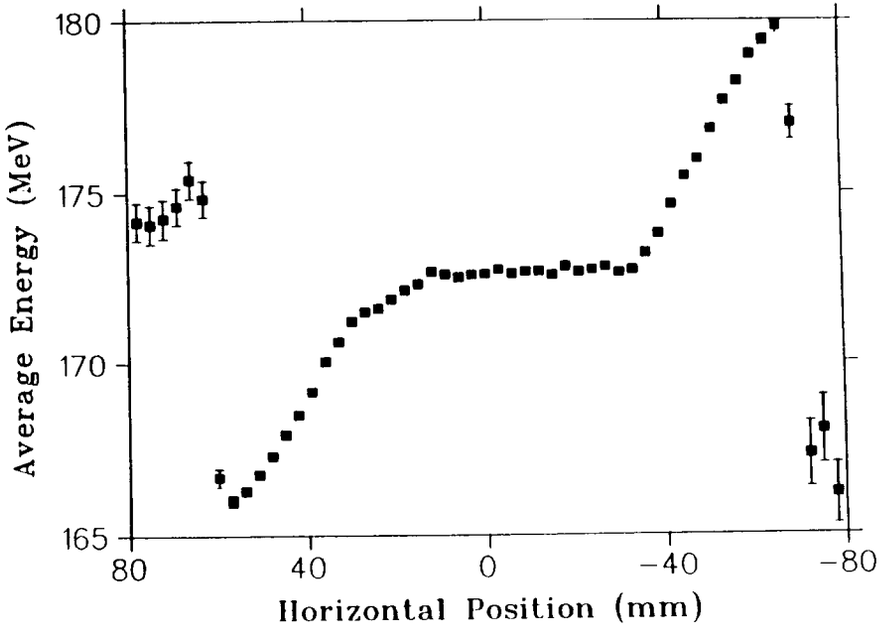

Fig. 4

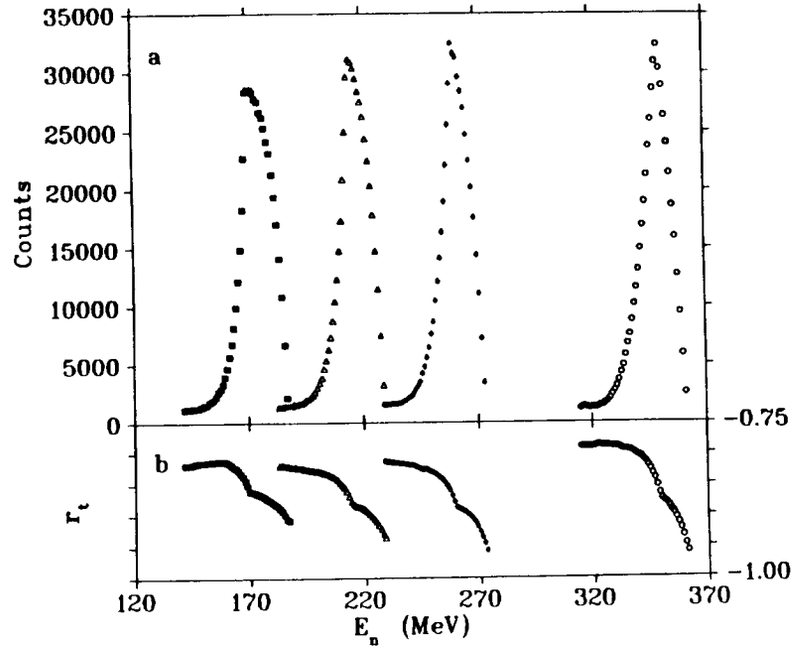

Fig. 5